Journal of Power Sources, 45 (1993) 291–301

Methanol oxidation and hydrogen reactions on NiZr in acid solution

C. C. Hays, R. Manoharan and J. B. Goodenough

Center for Materials Science and Engineering, ETC 9.102, University of Texas at Austin, Austin, TX 78712-1084 (USA)

(Received November 10, 1992; accepted in revised form March 1, 1993)

Abstract

The electrochemical properties of a $Ni_{50}Zr_{50}$ (at.%) alloy have been investigated by cyclic voltammetry and steady-state polarization measurements. The alloy forms a passivating oxyhydroxide film that makes it electrochemically stable in an acid solution. The oxyhydroxide film is shown to be an electrocatalyst for the methanol oxidation reaction (MOR). The reaction proceeds at surface O^{2-} ions neighboring a Ni^{3+} ion of a thicker passivating film; electron transfer from the surface to the electrode occurs diffusively by the nickel atoms of the film. A reaction pathway is presented that accounts for the observation of an optimum thickness for the passivating film. The NiZr alloy was also found to catalyze both hydrogen-oxidation and proton-reduction reactions (HOR and PRR) if it has a thinner surface oxyhydroxide film. The alloy appears to form mixed NiZrH and $NiZrH_{3-x}$ hydrides on cycling negative of the normal hydrogen potential. The activity of the hydrogen-oxidation reaction on a hydride surface was found to increase in the presence of streaming hydrogen gas and also with increasing negative initial potential. Although the hydride is unstable in acid, it may be an attractive candidate for use as a rechargeable negative electrode in an alkaline metal/air or nickel–metal hydride secondary battery.

Introduction

The increasing demand for alternative energy sources has lead to new strategy approaches in the design of catalytic materials [1, 2]. Two areas of great activity are the development of a practical methanol/air fuel cell [3] and the improvement of secondary batteries [4]. In a methanol/air fuel cell, one of the products of the methanol-oxidation reaction (MOR) at the cell anode is CO_2; if an alkaline electrolyte is used, the formation of carbonates at the anode is a serious problem. Thus, the methanol/air fuel cell must operate with an acid electrolyte, so the anode material must be stable in an acidic environment. At present, the most promising catalytic materials for the MOR are Pt-based alloys [5, 6]. However, the long-term chemical stability of the Pt-based alloys in an acid solution is questionable. Efforts to identify new catalytic materials have been halted primarily by corrosion problems due to the acidic environment.

One of the primary concerns associated with the Ni–Cd secondary battery is the environmental hazard posed by the use of Cd as the anode material. This concern has been eliminated with the development of the Ni–metal hydride (Ni–MH) battery [7]. Hydrogen insertion/extraction occurs reversibly at the MH anode. The positive electrode used is a standard Ni-oxyhydroxide material. The performance of the Ni–MH batteries has been proven in small battery sizes. The manufacturing methods employed

0378-7753/93/$6.00

in the Ni–MH technology are reported to be easily adapted to large-scale production [4]. Therefore, there is commercial interest in identifying the most suitable metal hydride for the anode.

In order to identify new electrode materials for these applications, we have initiated a study of binary alloys from Groups IV and VIII of the periodic table [3, 8]. In this paper electrochemical data for a $Ni_{50}Zr_{50}$ (at.%) alloy are presented that show the alloy's chemical stability and its MOR, proton-reduction reaction (PRR) and hydrogen-oxidation reaction (HOR) activities. These results are discussed in relation to the previous results for the MOR properties of a $Ni_{50}Ti_{50}$ (at.%) alloy. The data of this MOR study show that, in good agreement with those on NiTi, the reaction sites of the MOR on NiZr are not the bare-metal sites, but the surface O^{2-} ions of a thicker passivating oxyhydroxide film formed on the surface of the alloy upon application of anodic potentials. In the absence of a passivating film, or if the film is thin enough, the proton-reduction reaction (PRR) produces reversibly a metal hydride, and we monitor the HOR on the hydride surface with increasing thickness of the passivating film. The hydrides are not stable in 2.5 M H_2SO_4.

Experimental

The $Ni_{50}Zr_{50}$ (at.%) alloys were prepared in the form of small buttons by arc melting high-purity Ni (99.99%) and Zr (99.9%) under an argon atmosphere in a copper crucible. Generally, buttons with geometrical surface area between 3 and 5 cm^2 (2–5 grams) were prepared. The buttons were inverted and remelted several times to promote homogenization of the alloy. The weight loss after melting was less than 0.1% for each sample. To X-ray diffraction, the alloys were single-phase in the as-cast condition. The as-cast alloy samples did not require conventional heat treatment for homogenization because high cooling rates in the arc furnace resulted in a columnar sample microstructure. No measurable differences in chemical stability or electrochemical results were obtained for samples that were given a homogenizing heat treatment at 833 °C, which is two-thirds the melting temperature.

Electrochemical measurements were made in an all-glass, three-electrode cell. The NiZr alloy working electrodes were made by spot-welding a high-purity Ti (99.9%) wire to the alloy button. The spot-welded connection and Ti wire were separated from the electrolyte by encasing the connection/lead in an epoxy resin. A Pt wire formed into a loop was used as the counter electrode. A graphite-rod electrode was also used to check that no Pt from the counter electrode was being deposited on the working electrode. The reference was a Hg/Hg_2SO_4, SO_4^{2-} (2.5 M) electrode. The electrode potentials in this work are given with respect to the normal hydrogen electrode (NHE). The 2.5 M H_2SO_4 electrolyte was prepared with Analar grade H_2SO_4 and de-ionized water. The electrolyte was stirred continuously and purged with high-purity nitrogen gas to drive off any oxygen in solution. Cyclic voltammograms (CVs) were recorded with an EG&G model 273 potentiostat interfaced with an IBM PxT microcomputer controlled by a National Instruments IEEE-488 General Purpose Interface (GPIB) card. The EG&G HEADSTART™ Creative Electrochemistry software was used to drive the measurements, process the data, and display the CV. In the galvanostatic overvoltage measurements, the polarization currents were controlled with a constant-source d.c. power supply and the electrode potentials were measured with a digital voltmeter.

Results

Chemical stability of NiZr

The NiZr alloy was immersed in the 2.5 M H_2SO_4 working electrolyte for approximately two weeks. Except in a few cases where surface hydrides were formed, chemical analysis of the solution after immersion did not show any evidence of Ni or Zr species. Figure 1(a) shows CVs for NiZr in 2.5 M H_2SO_4 at 25 °C. The CVs do not show any dissolution region; the surface is passivated by the growth of an oxyhydroxide surface film. The anodic current decreases on successive cycles, curve (ii) of Fig. 1(a), because the thickness of the passivating film is fixed by the vertex potential; the film thickness increases with increasing vertex potential as can be seen by the onset of an anodic potential only after the vertex of the previous cycle is exceeded, Fig. 1(b). This behavior is typical of valve-metal CVs where no current is observed in the backward scan direction.

Methanol oxidation on NiZr

CVs of NiZr in 2.5 M H_2SO_4 at 25 °C both with (CV-a) and without (CV-b) methanol are shown in Fig. 2. In general, the CVs obtained on the addition of 1 M CH_3OH to the 2.5 M H_2SO_4 electrolyte show a large increase in current density at all potentials of the forward scan, and the increased current densities are due to the occurrence of the MOR. The magnitude of the current density, curve shape, and the occurrence of the MOR were dependent on the preparation of the alloy surface, number of previous cycles, and cycle potential range.

Over the potential range studied, the MOR activity increases as the potential increases; it decreases with number of cycles. Generally, it was found necessary to wait a period of time to recover the MOR activity after cycling. For surfaces that had been cycled a large number of times, it was necessary to wait for a period of 2 to 3 days with the sample immersed in the electrolyte to recover completely the MOR. The recovery time was always found to decrease in the presence of streaming hydrogen gas.

NiZr electrodes were then etched with a mixture of 5 ml HF, 25 ml HNO_3, and 50 ml H_2O to remove any oxyhydroxide film prior to a CV measurement. Figure 3 shows the anodic scan of such an initial CV obtained after application of a negative

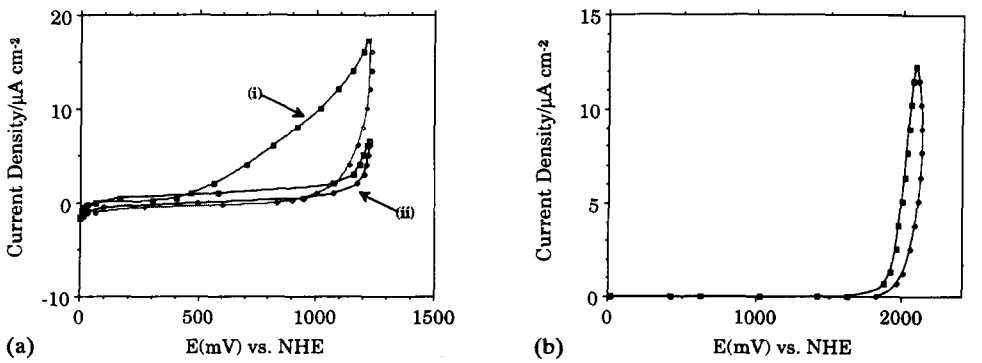

Fig. 1. Cyclic voltammograms for NiZr in 2.5 M H_2SO_4 and flowing N_2: (a) curve (i) is first cycle and (ii) is second cycle, and (b) typical $(n+1)$ cycle on increasing the vertex potential from its value in the nth cycle.

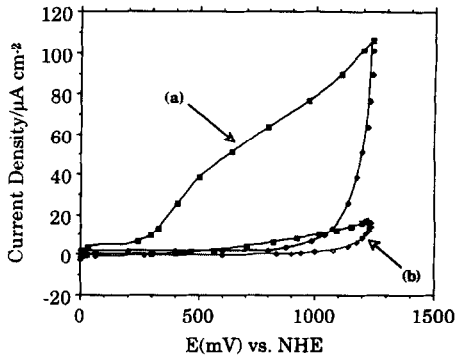

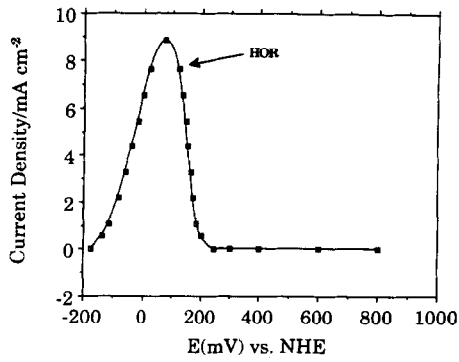

Fig. 2. Voltammograms for NiZr in 2.5 M H_2SO_4 and flowing N_2: (a) with 1 M CH_3OH, and (b) without 1 M CH_3OH.

Fig. 3. Cyclic voltammogram for chemically-etched NiZr sample in 2.5 M H_2SO_4 and flowing N_2 with 1 M CH_3OH.

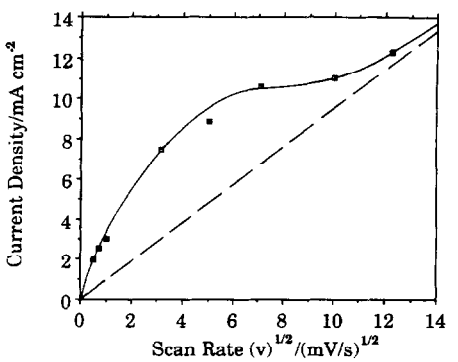

Fig. 4. HOR peak current density vs. (scan rate)$^{1/2}$.

anodic potential at 25 °C in 2.5 M H_2SO_4 in the presence of methanol and with nitrogen gas streaming through the electrolyte. No MOR is observed.

Hydrogen reactions on NiZr

The peak shown in Fig. 3 was identified as due to the HOR. To do this, a series of anodic scans were conducted at various negative initial potentials with nitrogen gas streaming through the electrolyte. As the initial potential became increasingly negative of the hydrogen potential ($E=0$), the amount of hydrogen extracted from the water increased, and the magnitude of the HOR-peak current density increased accordingly. Moreover, conducting the same series of CVs in the presence of hydrogen gas yielded a peak current density that was higher for each value of the initial potential; the hydrogen from the gas contributed to the HOR peak independently of the hydrogen extracted from the water.

Figure 4 shows the variation of the HOR-peak current density with the square root of the scan rates through the potential range −0.175 to +0.425 V. A single rate-limiting diffusion process would give a straight line [9]; the curve line indicates the presence of at least two processes, one of which is relatively slow.

Figure 5(a) shows the steady-state galvanostatic polarization curves for the oxidation of hydrogen on etched NiZr in 2.5 M H_2SO_4 at 25 °C with nitrogen and with hydrogen gas flowing, respectively, through the electrolyte solution. The polarization data were obtained after waiting for 2 to 3 minutes at each point. The increased current density observed in the presence of hydrogen gas confirms the occurrence of the HOR. The Tafel plots of Fig. 5(b) can be fitted to two straight lines; at higher current densities, the slopes are approximately 56 mV/decade for each data set. The Tafel slopes for the two lower current densities are 6 mV/decade for N_2 and 18 mV/decade for H_2 gas.

Some NiZr samples, when they were tested immediately after being taken from the arc-melting furnace, exhibited CVs as shown in Fig. 6. Again these CVs were conducted in 2.5 M H_2SO_4 with methanol at 25 °C in the presence of nitrogen gas. Figure 6(a) shows the occurrence of both the HOR and MOR, as labeled. The major HOR peak is off scale in Fig. 6(a) as the current range chosen for the potentiostat was too small. A minor oxidation peak, labeled NiOR, is seen to occur at a higher potential relative to the major HOR peak. Figure 6(b) shows the CV that immediately followed the first cycle shown in Fig. 6(a). In Fig. 6(b), all of the peaks have reduced current-density amplitudes. However, the HOR and NiOR peaks are clearly resolved. Continued cycling caused the disappearance of both these peaks (5 cycles). It is also

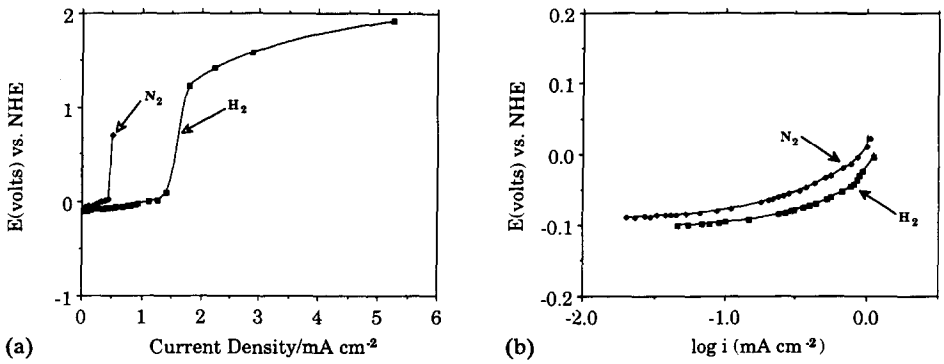

Fig. 5. Steady-state polarization for the HOR: (a) with/without hydrogen gas, and (b) showing only the Tafel regions.

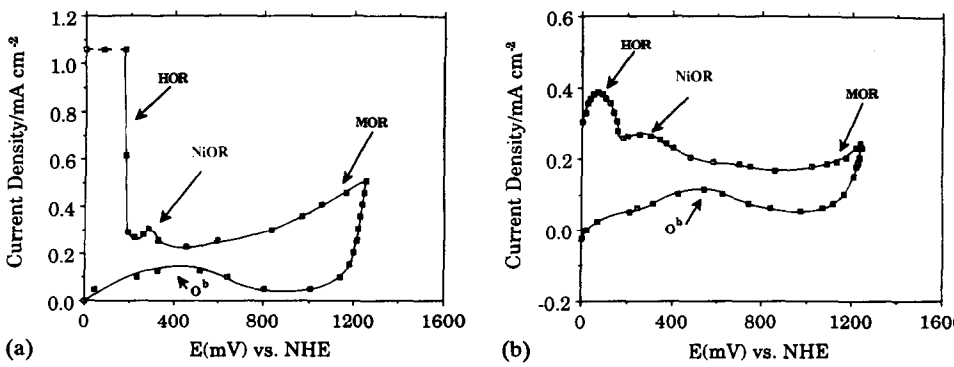

Fig. 6. Cyclic voltammogram for an as-cast NiZr sample: (a) first cycle, and (b) second cycle.

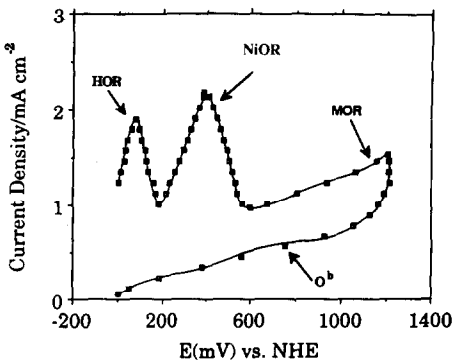

Fig. 7. Cyclic voltammogram for an as-cast NiZr sample: sample cycled ten times in the potential range 0 to 1625 mV, cyclic voltammogram taken after 24 h.

worth noting that the anodic oxidation peak O^b, which is normally observed during the backward scan on Pt electrodes in the presence of methanol, is also present in Figs. 6(a) and (b).

Following the CV of Fig. 6(b), the NiZr electrode was then cycled ten times in the potential range 0–1.625 V in order to prepare a thicker oxyhydroxide film on the sample surface. The sample was then left in the electrolyte for 24 h. Figure 7 shows the first CV conducted after this cycling procedure. The MOR showed increased activity with a peak current density $i_p = 1.73$ mA/cm^2 at $E = 1.2$ V. This value is greater than three times the MOR peak current density $i_p = 0.51$ mA/cm^2 shown in Fig. 6(a) at the same $E = 1.2$ V. In Fig. 7, the HOR also shows greatly increased activity with the HOR and NiOR peaks clearly resolved and with nearly equal magnitudes.

Discussion

Chemical stability

In acid solution, a nickel electrode corrodes over the potential range 0.3–0.6 V in an anodic voltage sweep by the dissolution of Ni^{2+} ions from the surface. $E_{th} = 0.6$ V is the threshold potential for conversion of the surface nickel to Ni^{3+} ions, which do not dissolve in acid. The Ni^{2+}-dissolution reaction does not occur at any potential in acid on the 50–50 (at.%) NiZr alloy; no dissolution peaks are observed in the CVs of Fig. 1, even though there is evidence that the metal atoms are diffusing into an aqueous surface layer to form an oxyhydroxide passivating surface film via the reactions:

$$Zr^0 + 2H_2O \longrightarrow ZrO_{2-x}(OH)_x + (4-x)H^+ + (4-x)e^- \quad (1)$$

$$Ni^0 + 2H_2O \longrightarrow NiO_y(OH)_{2-y} + (2+y)H^+ + (2+y)e^- \quad (2)$$

The oxidation state of the cations at the outer surface of the film can be expected to increase as the film thickness increases with the applied anodic potential. Apparently, the bridging by surface anions of a Ni^{2+} and a Zr^{4+} ion suppresses the Ni^{2+}-ion dissolution by shifting the dissolution potential above the threshold potential $E_{th} =$

0.6 V for conversion of surface Ni^{2+} to Ni^{3+} ions. Previous studies of RuTi have shown that the Ru corrosion potential is shifted anodically by about 0.34 V by alloying with Ti, and we have attributed suppression of the Ni^{2+}-ion dissolution reaction on NiTi to a similar anodic shift of the Ni^{2+}-ion dissolution reaction [3, 8].

Methanol oxidation on NiZr

The MOR begins with a dissociative chemisorption on the surface; adsorption on the surface oxygen species requires electron transfer from the CH_3OH molecule to the bulk electrode in the reaction:

$$CH_3OH + 2S \longrightarrow SCH_2OH + SH \tag{3}$$

where S is a surface atom. The absence of any MOR activity in the potential range $E \leq 0.25$ V (Fig. 2) and after etching the surface (Fig. 3) both indicate that the MOR is occurring on an oxyhydroxide surface layer and not on the bare alloy. Moreover, it is significant that for the thinner films, no MOR activity is observed until the potential exceeds 0.6 V, the threshold potential of Ni^{3+} ions. A similar behavior occurs on a pure-nickel electrode [3]. In the reverse scans of all the CVs, no reversal of the $Ni^{3+/2+}$ reaction is observed, and the MOR activity is found on subsequent anodic scans to begin at voltages $E > 0.25$ V. We deduce from these observations that surface Ni^{3+} ions must be present to catalyze the MOR.

At lower anodic potentials of the initial CV, the surface of an oxyhydroxide film contains only Ni^{2+} and Zr^{4+} ions; both the Ni^{2+}–Ni^{+} and Zr^{4+}–Zr^{3+} redox couples in the oxyhydroxide film have too high an energy to accept electrons from a CH_3OH molecule in the eqn. (3). However, the Ni^{3+}–Ni^{2+} redox energy lies well below that needed to accept electrons from a CH_3OH molecule, and the data support the following dissociative chemisorption reactions:

$$2Ni^{3+}O^{2-} + CH_3OH \rightleftharpoons Ni^{2+}OH^{-} + Ni^{2+}O^{-}CH_2OH \longrightarrow$$

$$Ni^{3+}O^{2-} + Ni^{3+}O^{-}C^{-}HO + 3H^{+} + 3e^{-} \tag{4}$$

$$Ni^{3+}O^{-}C^{-}OH \longrightarrow Ni^{3+}O^{-}C^{-}=O + H^{+} + e^{-}$$

in which equilibrium with the pH of the electrolyte retains a nearly fixed surface charge on the electrode. Moreover, the equilibrium reaction:

$$Ni^{3+}O^{-}C^{-}=O \rightleftharpoons Ni^{2+}O^{-}C^{\cdot}=O \tag{5}$$

allows the reaction to go to completion:

$$Ni^{2+}O^{-}C^{\cdot}=O + H_2O \longrightarrow Ni^{2+}O^{-}COOH + H^{+} + e^{-}$$

$$Ni^{2+}O^{-}COOH \longrightarrow Ni^{2+}OH^{-} + CO_2\uparrow \tag{6}$$

$$Ni^{2+}OH^{-} \longrightarrow Ni^{3+}O^{2-} + H^{+} + e^{-}$$

According to this reaction schema, methanol oxidation at the surface of an oxyhydroxide passivating film requires three features:

(i) electron transport across the film, which is also necessary for film formation and growth according to eqns. (1) and (2);

(ii) formation of a surface acceptor oxidation state M^{m+} without the intermediary of an $M^{(m-1)+}$ dissolution reaction, which is made possible on NiZr by the coexistence of Zr^{4+} and Ni^{2+} ions in the films and the accessibility of Ni^{3+} species at the surface of films still thin enough to support reasonably rapid charge transfer across the film, and

(iii) an equilibrium reaction like (5), which makes possible extraction of oxygen from the water of the electrolyte provided reaction (6) is rapid enough to drive reaction (5) to the right.

On NiZr, the rate of the first step in reaction (6) depends on the film thickness as do all those reactions in (4) and (6) that involve electron transfer across the film. Electron transfer can only be between Ni^{3+} and Ni^{2+} ions as it is not possible to reduce either Zr^{4+} or Ni^{2+} at the potentials used in this study. Since electron transfer from Ni^{2+} to Ni^{3+} is diffusive within an oxyhydroxide layer, it is relatively slow at room temperature. Because the creation of Ni^{3+} requires a film thickness greater than a critical value, there is an optimum film thickness for the overall reaction near the critical thickness for conversion of surface Ni^{2+} to Ni^{3+} ions, which can explain why the MOR activity not only requires a critical film thickness for its onset, but also decreases with increasing film thickness on successive CV cycles.

In general, an oxyhydroxide equilibrium film thickness can be expected to increase with the applied potentials by about 20 Å/V [10]. The film thickness grows on repeated cycling to the same vertex potential because of the poor room-temperature mobility of the cations in the oxyhydroxide layer; the MOR activity increases with time at the vertex potential until the optimum film thickness is reached. Reduction of the film thickness occurs in the absence of an applied voltage, but only over a period of days unless in the presence of streaming hydrogen gas.

Hydrogen reactions on NiZr

The 50–50 (at.%) NiZr alloy is an excellent hydrogen-storage material. Libowitz *et al.* [11, 12] have shown that two hydride phases, NiZrH and $NiZrH_{3-x}$ with $x<0.5$, are stable; they can be formed by either chemical or electrochemical reactions on a NiZr surface. However, their formation is inhibited in the presence of a passivating oxyhydroxide surface film.

In our experiments, etched and as-cast NiZr surfaces formed hydrides at potentials negative of the NHE. In contrast to the hydrides of NiTi and RuTi alloys, the brittle hydride phases proved to be unstable in the 2.5 M H_2SO_4 electrolyte. If the electrode was left in the solution for several days after hydride formation, the Ni^{2+}-dissolution reaction turned the color of the electrolyte blue/green; also, the hydride films formed on the alloy surface spalled off and fell to the bottom of the electrochemical cell. X-ray diffraction of the bittle material scraped off the surface and added to that collected from the bottom of the cell showed it to be a mixture of hydride and oxide phases. It would appear that the hydrogen of the hydride inhibits the formation of the passivating oxyhydroxide film, probably by suppressing the formation of Zr^{4+} ions.

With a few NiZr samples, we noted the formation of hydride surface phases followed by Ni^{2+}-ion dissolution in 2.5 M H_2SO_4 after only a simple immersion in the electrolyte with no applied potential. However, most samples were stable, being passivated by a thin oxyhydroxide surface film.

In the experiment of Fig. 3, etched NiZr electrodes were first loaded with hydrogen by the application of a potential $E<0$ to form a hydride. The absence of any MOR activity in Fig. 3 is striking; even repeated cycling failed to induce any MOR activity. The passivating oxyhydroxide film needed for the MOR does not form on the hydride surface, at least in the time for a cycle. Chemical etching of the surface after these measurements always yielded a considerable amount of gas not observed on etching the virgin alloy prior to these measurements; the amount of gas evolved indicated that a sizable fraction of the sample had formed a hydride phase.

The CVs used to obtain Fig. 4 all exhibited only one HOR peak like that of Fig. 3; this peak typically had full width at half-maximum of $\Delta E = 180$–200 mV and a peak potential of $E_p = 75$ mV. On a hydride surface, the HOR has two sources of atomic hydrogen, bulk hydrogen from the hydride and surface hydrogen from hydrogen gas in the electrolyte that is residual from the PRR and may also be supplied in a gas stream. Since the diffusion coefficient for bulk hydrogen can be expected to be significantly slower than that of hydrogen gas in the electrolyte, the evidence in Fig. 4 for two quite different diffusion-controlled reaction rates is to be expected. The Tafel slopes of Fig. 5 also indicate the presence of two different diffusion rates for the species being oxidized.

The onset potential for a HOR process on a hydride surface reflects the stability of the hydride. The onset potentials on hydrated NiZr are 0.1 to 0.2 V negative of the NHE, see Figs. 3 and 5, which reflects a greater stability of the H–H bond of gaseous hydrogen relative to the M–H bond of the alloy at $E = 0$ V. In the case of hydrated RuTi, a sharp HOR peak is found at $E = 0.65$ V, which indicates a more stable hydride. An even greater stability of the hydrides of NiTi suppresses the appearance of the HOR peak in the voltage range of a conventional CV.

Figures 6 and 7 demonstrate that thinner passivating films allow hydrogen penetration to the alloy surface to form a thin surface-hydride layer on the cathodic sweep; on the anodic sweep, the hydrogen of the thin hydride layer is removed, which allows the formation and build-up of the oxyhydroxide layer on successive cycling. The thicker the oxyhydroxide film, the more the HOR and NiOR peaks are suppressed. The more negative HOR peak, which is characteristic of the hydride surface, is suppressed first as the second NiOR peak first builds up and then is, in its turn, suppressed. At potentials $E > 0.6$ V, the MOR sets in. On the backward sweep, an oxidation peak O^b is observed.

The inability to reduce either the Ni^{2+} or the Zr^{4+} ions of the passivating film on NiZr makes thicker films block proton transfer to the alloy surface to form hydride at the potentials used in these experiments. This behavior contrasts with that of the thicker passivating films on NiTi and RuTi, which do not block hydride formation; the Ti-3d band does accept electrons near the NHE potential to charge–compensate for H^+ ions diffusing from the surface of the passivating film to the bulk alloy:

$$Ti^{4+}O^{2-} + e^- + H^+ \longrightarrow Ti^{3+}OH^- \tag{7}$$

followed by the proton-transfer reaction within the film:

$$Ti^{4+}O^{2-} + Ti^{3+}OH^- \longrightarrow Ti^{3+}OH^- + Ti^{4+}O^{2-} \tag{8}$$

This mechanism is not operative in NiZr so long as neither Zr^{4+} nor Ni^{2+} ions are reduced. However, for a thin passivating film, electrons may tunnel across this passivating film from the alloy to adsorbed protons, and reduction of a surface proton allows it to be transferred as a neutral hydrogen atom across the film to form the hydride.

We suggest that the peak NiOR corresponds to the surface reaction:

$$Ni^0(OH_2)_2 \longrightarrow Ni^{2+}(OH^-)_2 + 2H^+ + 2e^- \tag{9}$$

since the formation of an oxyhydroxide passivating film is suppressed on the hydride where the HOR peak is found and the NiOR activity is completed by $E = 0.6$ V where Ni^{2+} is converted to Ni^{3+}. The MOR occurs on the passivating film containing Ni^{3+}; it reaches its highest values where the film thickness just exceeds that needed to convert Ni^{2+} to Ni^{3+}.

The oxidation peak O^b observed on the backward sweep is similar to that observed on Pt and NiTi electrodes in the presence of methanol; we have discussed this peak elsewhere [3]. As in the case of the passivated NiTi alloy, O^b is due to the chemisorption reaction (4), which becomes too slow to be visible on thicker oxyhydroxide films on NiZr. Electron transfer across the passivating film on NiTi is strikingly more rapid [3] because the Ti-3d states are accessible; there is no reduction of either the Zr^{4+} or the Ni^{2+} ions of the films on NiZr.

Conclusions

We have shown that the 50–50 (at.%) NiZr alloy is stable in 2.5 M H_2SO_4 provided hydride formation is suppressed and that stabilization is due to the formation of a surface oxyhydroxide film having an equilibrium thickness that increases with an applied potential $(E-E^0)<0$, where E^0 is the potential of the NHE reference. Stabilization is achieved by suppression of the Ni^{2+}-dissolution reaction that occurs on a nickel electrode in the range of 0.3 to 0.6 V versus NHE. Hydride formation occurs where electrons can tunnel from the bare alloy surface to electrolyte protons at a potential $(E-E^0)<0$; the hydrides are brittle, they suppress formation of the oxyhydroxide film, and they corrode in 2.5 M H_2SO_4.

We have demonstrated the occurrence of the MOR on the passivating oxyhydroxide surface films of a NiZr electrode, the HOR on the surface of a hydrided NiZr electrode, a Ni^0 to Ni^{2+} reaction NiOR on an oxyhydroxide film too thin to contain Ni^{3+} ions, and also a PRR that results in hydride formation provided any passivating oxyhydroxide film on the surface is not too thick.

We have shown indirectly that the MOR takes place on an oxyhydroxide surface thick enough to contain surface Ni^{3+} ions, and we have presented a schema for the reaction pathway that conforms qualitatively to all the data: it begins with dissociative chemisorption at oxygen atoms neighboring a Ni^{3+} ion.

We have also shown that there is an optimum passivating-film thickness for the MOR; it is the minimum thickness compatible with a large Ni^{3+}-ion concentration at the surface because electron transport via nickel atoms across a film limits the rate of the reaction that must compete in the equilibrium reactions of eqns. (4) and (6).

These findings suggest that there may be other oxyhydroxide films supporting faster electron transport that not only passivate a transition-metal electrode surface, but also catalyze a more active MOR in the presence of a transition-metal cation of higher oxidation state. Moreover, the reversible hydrogen insertion/extraction reaction may make NiZr an attractive candidate for an anode in an alkaline metal/air or Ni–MH secondary battery.

Acknowledgement

The financial support of the Robert A. Welch Foundation, Houston, TX, USA, is gratefully acknowledged.

References

1 R. Manoharan and J. B. Goodenough, *Proc. 26th Intersoc. Energy Conversion Eng. Conf., 3* (1991) 552.
2 *Ext. Abstr. of Battery Division, Fall Meet. Electrochemical Society, Phoenix, AZ, USA, 1991.*
3 R. Manoharan and J. B. Goodenough, *J. Mater. Chem., 2* (1992) 875.

4 S. Venkatesan, M. A. Fetcenko, S. K. Dar and S. R. Ovshinsky, *Proc. Intersoc. Energy Conversion Eng. Conf., 3* (1991) 435.
5 R. Parsons and T. Van der Noot, *J. Electroanal. Chem., 257* (1988) 9.
6 D. S. Cameron, G. A. Hards, B. Harrison and R. J. Potter, *Platinum Met. Rev., 31* (1987) 177.
7 J. B. Goodenough, R. Manoharan, A. K. Shukla and K. V. Ramesh, *Chem. Mater., 1* (1989) 391.
8 R. Manoharan and J. B. Goodenough, *Electrochim. Acta, 36* (1991) 19.
9 A. J. Bard and L. R. Faulkner (eds.), *Electrochemical Materials: Fundamentals and Applications,* Wiley, New York, 1980.
10 I. Young (ed.), *Anodic Oxide Films,* Academic Press, New York, 1961.
11 G. G. Libowitz, in G. G. Libowitz and M. S. Whittingham (eds.), *Material Science in Energy Technology,* Academic Press, New York, 1979.
12 G. G. Libowitz, H. F. Hayes and T. R. P. Gibb Jr., *J. Phys. Chem., 62* (1958) 76.